Effect of modulation of the swirl ratio and gas and liquid flow rates on the structure of the spray produced by a two-fluid coaxial atomizer

A. Aliseda*, R. Osuna-Orozco, P.D. Huck, N. Machicoane
Department of Mechanical Engineering, University of Washington, USA

Abstract

The effect of harmonically oscillating the gas swirl ratio, and the liquid and gas flow rates on the droplet size and number density distributions is experimentally studied. A coaxial two-fluid atomizer with laminar liquid and turbulent gas streams is investigated using high-speed video shadowgraphy, as well as interferometric droplet size and velocity measurements. The liquid mass loading is kept small ($0.1 < m < 0.55$), while the gas momentum ratio, M, is varied from 5 to 125. The swirl ratio (the ratio of the gas flow rate injected into the atomizer nozzle with angular momentum to the gas flow rate injected without angular momentum) ranges from zero to one. The flow rates are perturbed via harmonic forcing of the gas and liquid injection rates. The effect of the flow rate modulation frequency and amplitude, on both the spray primary instabilities and the droplet spatial distribution are characterized. We also investigate how the swirl ratio can be used to finely tune external perturbations, aimed at achieving better spray control. The laminar liquid stream is charged by the strong local electric field created between the metallic injection needle used as the anode, and a ring located on the streamwise end of the coaxial gas chamber used as the cathode. The electric charge in the liquid depends on the liquid and gas flow rates, and affects the primary instabilities, thus feeding into the variables modulated in the overall spray control strategy.

Introduction

Break-up of a liquid jet by a high speed coaxial gas jet is a frequently-used configuration to generate a high quality spray. Despite its widespread application in engineering and natural processes, the instabilities that control the liquid droplet size and their spatio-temporal distribution in the spray are not completely understood. Fundamental understanding of the mechanisms that dominate ligament formation and break-up in the liquid, as well as those that determine the differential transport of droplets in the spray can provide quantitative design and analysis tools for spray engineering.

The liquid break-up process is known to follow a cascade of instabilities which, at high gas Reynolds numbers and gas to liquid momentum ratios, are dominated by a Kelvin-Helmholtz instability driven by the shear between the low speed liquid and high speed gas streams and a subsequent Raleigh-Taylor instability driven by the acceleration of the liquid-gas density interface[1]. The effect of unsteadiness in the liquid or gas streams is, however, not known. Because there are multiple characteristic time scales in the break-up process, it is not possible to predict *a priori* what are the effective frequencies that will significantly affect the atomization process beyond the obvious quasi-steady change in gas-to-liquid momentum ratio.

This paper studies the effect that harmonic oscillations have on the atomization instabilities, as well as on the resulting spray structure. High speed video of the flow near the nozzle (near field), as well as of the mid field where break-up is complete, is shown and quantitative analysis allows for general understanding of the physics controlling the atomization under this set of conditions.

Experimental Methods

The study is conducted using a canonical two-fluid coaxial atomizer designed and constructed at the University of Washington Multiphase Flow Lab. The goal is to create a standard two-fluid coaxial atomizer capable of producing efficient atomization over the widest possible ranges of liquid and gas Reynolds numbers, with resulting ranges of Weber number, mass and momentum ratios and swirl ratio (between the angular and non-angular momentum gas streams). This canonical atomizer is also being investigated using radiographic measurements [2, 3, 4] and computational simulations [5] by our colleagues and us in the context of an ONR MURI to develop Spray Control based on first principles understanding and modeling. CAD drawings and detailed construction blueprints are available at the MURI Spray Control website: http://blogs.cornell.edu/spraycontrolmuri and at http://fluids.me.washington.edu. A sketch of the atomizer, with a representative shadowgraph image of liquid atomization at high gas Reynolds number and gas-to-liquid momentum ratio can be seen in figure 1 (see [6] for more details on the design and the atomizer characterization).

*Corresponding author: aaliseda@uw.edu

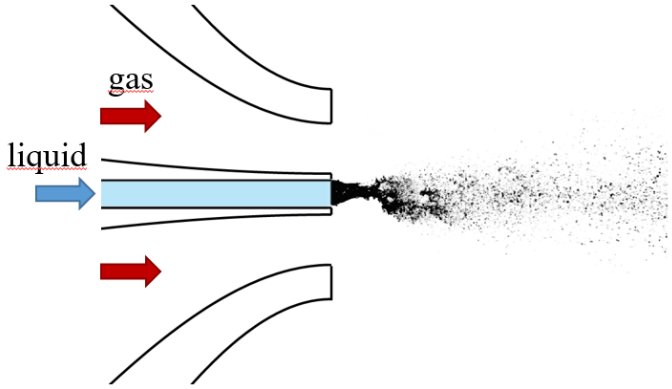

Figure 1. Sketch of the canonical two-fluid coaxial atomizer designed and manufactured for this study. Detailed construction drawings of the atomizer are available from the MURI Spray Control website: http://blogs.cornell.edu/spraycontrolmuri/

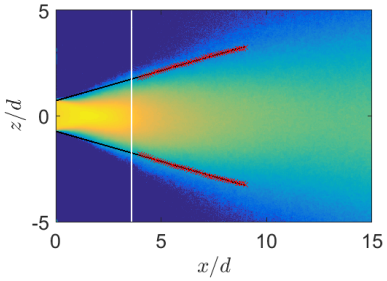

Figure 2. Visualization of the Spray Structure at $Re_g = 4\ 10^4$. Mean intensity field at the highest liquid flow rate, phase $\phi = 0$ within the harmonic oscillation, showing the spray spreading rate from the 2σ intensity cutoff on a Gaussian fit to the radial evolution of the intensity, for different distances downstream of the nozzle.

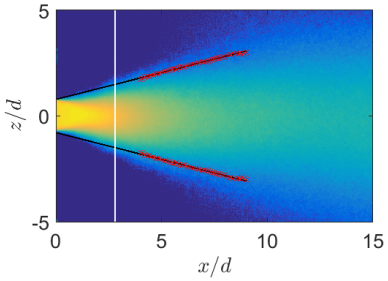

Figure 3. Visualization of the Spray Structure at $Re_g = 4\ 10^4$. Mean intensity field at the average liquid flow rate, phase $\phi = \pi/2$ within the harmonic oscillation, showing the spray spreading rate from the 2σ intensity cutoff on a Gaussian fit to the radial evolution of the intensity, for different distances downstream of the nozzle.

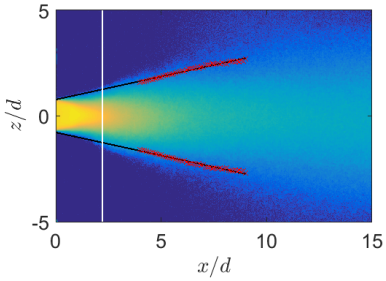

Figure 4. Visualization of the Spray Structure at $Re_g = 4\ 10^4$. Mean intensity field at the lowest liquid flow rate, phase $\phi = \pi$ within the harmonic oscillation, showing the spray spreading rate from the 2σ intensity cutoff on a Gaussian fit to the radial evolution of the intensity, for different distances downstream of the nozzle.

High speed video of light propagation across the spray (back-lighting) is collected for a wide range of experimental conditions (Gas Reynolds numbers from $10^4 - 2\ 10^5$, Weber number based on the gas exit velocity and liquid jet diameter[7] $We = \rho_g U_g^2 d_l/\sigma = 10 - 10^4$). The liquid Reynolds number is kept within laminar conditions inside the liquid injection duct prior to the nozzle, $Re_{liquid} = 1,000 \pm 500$.

An LED monochromatic light panel is used to provide parallel illumination for the spray. The axis of the light is coaxial with the camera lens and the region of interest imaged is quasi-uniformly (less than 10% change in background intensity without the spray present). Image sequences are collected at 10,000 frames per second, for one second at each condition studied. Light intensity maps, both mean and standard deviation, are quantitatively analyzed to obtain measures of the intact length of the liquid jet (extent of the primary break-up region) and the spray spreading angle. While these measures are influenced by thresholding choices that can be subjective, consistent use of the analysis, including the threshold choices, across the different cases studied here, with and without harmonic oscillation of the injection flow rates, allow for homogeneous comparison of the physics involved in the atomization processes studied. Additionally, comparison of the light attenuation measurements against X-ray attenuation, which can be objectively correlated to the Equivalent Path Length of liquid across the spray, collected at the Advanced Photon Source within Argonne National Lab, allows us to calibrate this optical measurements and provide confidence in the characterization obtained, despite the subjective choice of thresholds in the analysis.

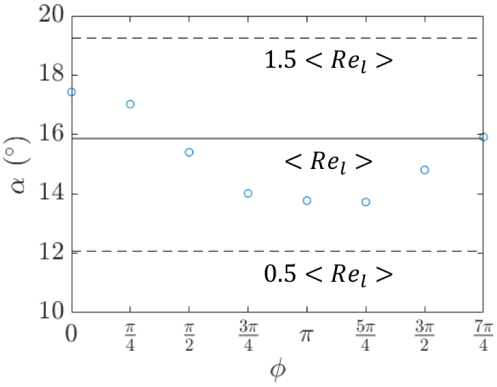

Figure 5. The Spray Angle evolution over the period of the harmonic oscillations as a function of the phase. The instantaneous Spreading Angle measured in the unsteady case is compared against the steady Spreading Angle for the average liquid flow rate (solid line) and at steady flow rates equal to the maximum and minimum liquid injection rates used in the harmonic oscillations (dashed lines).

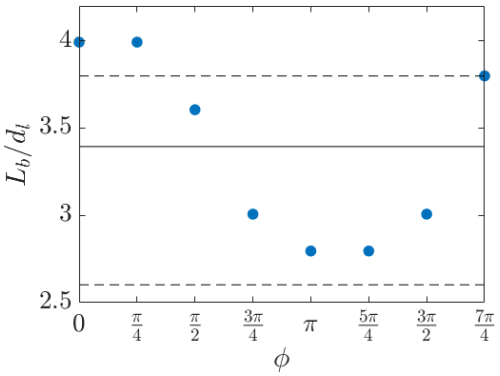

Figure 6. The Average Intact Length Time Evolution plotted as a function of the phase of the harmonic oscillatory liquid injection. The unsteady measurements are compared against the intact length measured for the average liquid flow rate injected (solid line) and the steady intact length measurements for the maximum and minimum liquid injection rates used in the harmonic oscillations (dashed lines).

Results and Discussion

The structure of the spray near-field is characterized from imaging of the light intensity attenuation by the spray. Figures 2, 3 and 4 show three representative images of the spray structure during harmonic oscillations at Reynolds numbers $Re = 4\ 10^4$ and amplitude of the liquid forcing 50% of the base liquid flow rate ($Re_{liquid} = [500, 1500]$). The peak flow rate phase, fig 2, causes the widest spray, consistent with the highest liquid injection and higher droplet density spreading further out radially. The average peak flow rate phase, fig 3, shows a spray that is similar, albeit narrower, to the steady spray spreading angle for the average flow rate. Finally, the minimum flow rate phase, fig 4, presents the narrowest spray, consistent with the minimum of liquid injected, but still significantly wider than the steady spray at the same instantaneous liquid injection ($Re_{liquid} = 500$). Figure 5 shows the deviation from quasi-steady behaviour in the spreading angle, highlighting that the unsteadiness causes moderate spray spreading that is bounded by the spreading angle values measured for the steady spray at equivalent liquid flow rates. That is, the spreading angles found within the harmonic oscillations are themselves harmonic in their time dependency but stay closer to the average value, with the range of oscillations being about half the extremes found in the steady cases for the maximum and minimum flow rates used as the amplitude of the input oscillations.

The impact of fluctuations in the liquid flow rate injected into the nozzle, oscillating harmonically at a fre-

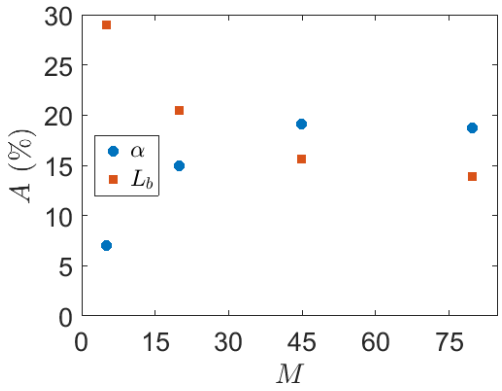

Figure 7. Amplitude of the effect of liquid flow rate fluctuations ($(max-min)/average$) on the Intact Length (L_b in red) and Spreading Angle (α in blue). Dependency of the effect of flow rate modulation with the Gas-to-liquid momentum ratio (M).

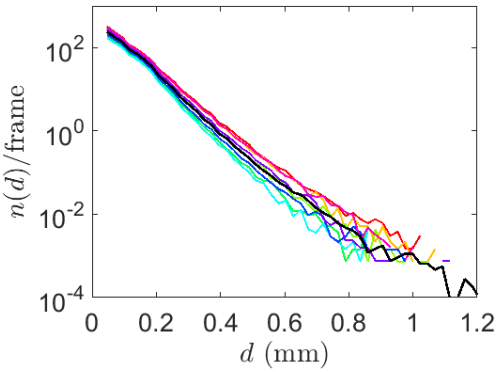

Figure 8. Droplet probability density function (in number of droplets per frame). The black line shows the pdf for steady conditions, while the blues/greens show the pdf for the phases within the harmonic oscillation during which the liquid flow rate is below the average, and the yellow/red show the pdf for the phases when the liquid flow rate is above average.

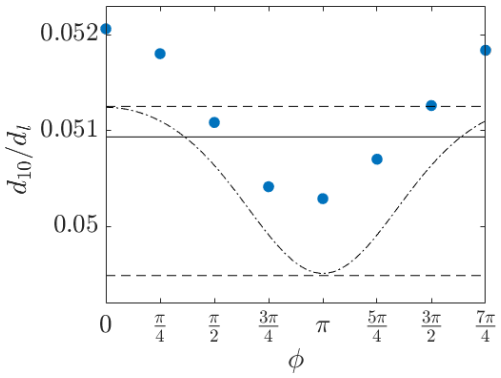

Figure 9. Average Droplet Diameter (D_{10}) as a function of phase within the harmonic oscillatory modulation of the liquid flow rate. The dashed lines represent the steady values obtained from experiments at constant liquid flow rates equal to the maximum (top) and minimum (bottom) flow rates used in the harmonic oscillations. The dot-dashed line is a harmonic (cosine) fit assuming quasi-steady behaviour.

quency of 1 Hz, on the Liquid Jet Intact Length is shown in figure 6. The values for steady state injections at the mean (solid) and max/min (dashed) liquid flow rates are shown for comparison. The Intact Length follows a harmonic evolution at the same frequency as the injection, and in phase with this input, but the magnitude of the effect goes above the steady values: the average intact length in the presence of fluctuations is higher than the value for a constant flow rate equal to the average, and the maximum and minimum intact lengths are both larger than the intact lengths found under steady conditions corresponding to the maximum and minimum flow rates used in the harmonic fluctuations.

Increasing the Gas-to-liquid Momentum Ratio greatly reduces the impact of liquid-flow-rate fluctuations, as measured by the amplitude of the resulting oscillations in liquid Intact Length. The effect on the Spreading Angle, however, is the opposite: as M increases, the amplitude of the Spreading Angle fluctuations increases. This can be seen in the measurements in figure 7. It can be explained by the stochastic nature of the Spreading Angle measurements which, unlike the Intact Length where the measurement detects the location occupied by liquid most of time, depends on the location where a few droplets can be found over the time sequence imaged. Because it is tuned to detect rare events, as the Gas Reynolds increases and the turbulent large structures increase in size and frequency, the droplets in the spray are carried more towards the edges of the jet, therefore impacting the pdf as a wide tail of the light intensity attenuation and increasing the spreading angle based on events that only happen when the liquid flow rate is around the peak.

The effect of harmonic oscillations on the formation of droplets after atomization is shown in figures 8 and 9. In figure 8, the number of droplets of a given size is averaged for all the images collected at the same phase of the harmonic oscillations. This probability density function phase-averaged with the input excitation shows a lower probability of large droplets (green/blue lines) for the time intervals when the liquid flow rate was smaller than the average (shown for reference as the black line), while the probability for large droplets increases (yellow/red lines) above that formed by the mean flow (in black). The same statistical trend is shown in the following figure, figure 9, but with just one numerical value: the arithmetic average droplet diameter. The blue dots indicate the values of D_{10} for the different phases within the harmonic oscillation of the liquid flow rate, with a clear trend towards smaller droplets (lower D_{10}) for the low flow rates phases of the period and larger droplets (higher D_{10}) for the phases with high flow rate. The experimental dots follow the same trend, but are always above the dashed line that indicates the expectation for average droplet diameters if the process of droplet formation was quasi-steady and the droplets formed during the harmonic oscillations where the same as those measured at steady-state for the same input values of liquid and gas flow rates.

The "controllability" of the droplet diameter by harmonic oscillations in the liquid flow rate is presented in figures 10 and 11. The trend is to increase the range of sizes accessible to the atomizer by a control strategy that consists of oscillating flow rates as the gas momentum available to break the liquid increases. This is consistent with the observation made in variability with an increase in figure 7 that the spreading angle increases with gas-to-

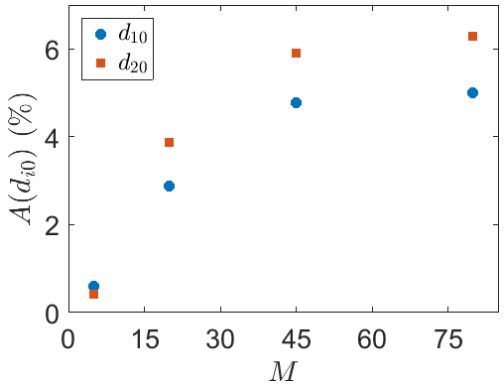

Figure 10. The amplitude of the variation in the droplet average diameter (arithmetic mean, D_{10}, and surface-area average, D_{20}) as a function of the gas-to-liquid momentum ratio, M.

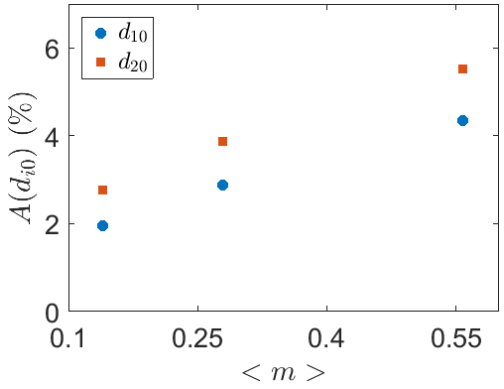

Figure 11. The amplitude of the variation in the droplet average diameter (arithmetic mean, D_{10}, and surface-area average, D_{20}) as a function of the liquid-gas mass ratio, m.

liquid momentum ratio. As the turbulent structures gain in amplitude and frequency, the break-up process results in higher variability in the size of the droplets, as well as in more energetic motions of the droplets after break-up that take them further radially extending the edges of the spray. The opposite trend is observed with the liquid mass loading. While always low and playing a small role in the break-up dynamics, as the liquid mass injected increases (m increases at constant gas injection), the amplitude of the variation in droplet diameter increases. The possibility that the instantaneous value of the mass loading, m, reaches a critical value in which it starts to hinder the break-up process is higher as the mean value of m is closer to unity. When the harmonic oscillations are in the part of the period where the value is higher than the average, m can reach values close to 0.7-0.8 and the droplet size will increase significantly compared to the droplets formed when m is close or below the mean of 0.55. Thus, harmonic oscillations close to the non-linear regime in which a small increase in m does play a big role in break-up (in this case increasing the size of the droplets as the energy transfer from the gas is not sufficient to completely atomize the liquid jet), result in high variability from small control inputs. More analysis needs to quantify this trend and resolve the limit in which the droplet sizes are too large to be practically useful in this non-linear regime.

Summary and Conclusions

The first step in developing a close-loop feedback control algorithm for a two-fluid coaxial atomizer has been conducted experimentally. High Speed Video quantitative visualizations have been used to measure the structure of the spray produced in this canonical atomizer configuration under steady and harmonically forced liquid and gas flow rates. The important non-dimensional parameters that control the modes of atomization under the conditions studied, namely the mass (m) and momentum ratios (M) of the two fluid streams, have been explored. Further research on the liquid Weber number effect, changing the surface tension in the liquid stream will be explored to analyze the whole range of spray working fluids of interest.

The results show the importance of the unsteadiness in the spray dynamics in contrast with the quasi-steady measurements collected for the entire range of harmonic oscillations but keeping the flow rates constant for long times (minutes) between acquisition. This work is a requisite characterization of the open loop harmonic forcing, and enables the use of the extensive quantitative information obtained, in the form of an input-to-output transfer function, to transitioning to a full feedback control algorithm. These measurements will be used in reduced order modeling of the spray and inform Adjoint models of the system to identify parameter sensitivity and optimal location of discrete points for actuation and sensing.

Acknowledgements

This work was sponsored by the Office of Naval Research (ONR), as part of the Multidisciplinary University Research Initiatives (MURI) Program, under grant number N00014-16-1-2617. The views and conclusions contained herein are those of the authors only and should not be interpreted as representing those of ONR, the U.S. Navy or the U.S. Government.

References

[1] Aliseda, A., Hopfinger, E. J., Lasheras, J. C., Kremer, D. M., Berchielli, A., Connolly, E. K., *International Journal of Multiphase Flow* 34(2):161-175 (2008).

[2] Bothell, J. K., Li, D., Morgan, T. B., Heindel, T. J., Aliseda, A., Machicoane, N., Kastengren, A., *14th Triennial International Conference on Liquid Atomization and Spray Systems*, Chicago, Illinois, July 22-26, 2018.

[3] Li, D., Bothell, J. K., Morgan, T. B., Heindel, T. J., Aliseda, A., Machicoane, N., Kastengren, A., *14th Triennial International Conference on Liquid Atomization and Spray Systems*, Chicago, Illinois, July 22-26, 2018.

[4] Morgan, T. B., Bothell, J. K., Li, D., Heindel, T. J., Aliseda, A., Machicoane, N., Kastengren, A., *14th Triennial International Conference on Liquid Atomization and Spray Systems*, Chicago, Illinois, July 22-26, 2018.

[5] Vu, L. X., Chiodi, R., Desjardins, O. *14th Triennial International Conference on Liquid Atomization and Spray Systems*, Chicago, Illinois, July 22-26, 2018.

[6] Huck P., Machicoane N., Osuna-Orozco R., Aliseda A., *14th Triennial International Conference on Liquid Atomization and Spray Systems*, Chicago, Illinois, July 22-26, 2018.

[7] Varga, J. C., Hopfinger, E. J., Lasheras, J. C., *Journal of Fluid Mechanics*, 497:405-434 (2003).